JOURNAL OF Materials CHEMISTRY

Structure of $(Ta_2O_5)_x(SiO_2)_{1-x}$ xerogels ($x=0.05$, 0.11, 0.18, 0.25 and 1.0) from FTIR, ^{29}Si and ^{17}O MAS NMR and EXAFS

David M. Pickup,*[a] Gavin Mountjoy,[a] Mark A. Holland,[a] Graham W. Wallidge,[b] Robert J. Newport[a] and Mark E. Smith[b]

[a]*School of Physical Sciences, University of Kent at Canterbury, UK CT2 7NR. E-mail: dmp@ukc.ac.uk*
[b]*Department of Physics, University of Warwick, Coventry, UK CV4 7AL*

Received 3rd February 2000, Accepted 15th June 2000
Published on the Web 14th July 2000

A combination of ^{29}Si and ^{17}O MAS NMR, EXAFS and FT-IR spectroscopy has been used to study the atomic structure of $(Ta_2O_5)_x(SiO_2)_{1-x}$ ($x=0.05$, 0.11, 0.18 and 0.25) xerogels prepared by reacting partially-hydrolysed tetraethyl orthosilicate with tantalum(v) ethoxide. Amorphous tantala, a-Ta_2O_5, xerogels have also been prepared and their structures studied in detail for the first time. Results have shown that in all these materials, Ta adopts predominantly 5-fold coordination with respect to oxygen. For the mixed oxide xerogels, partial phase separation of the two component oxides occurs for $x>0.11$.

Introduction

$(Ta_2O_5)_x(SiO_2)_{1-x}$ mixed oxide materials have attracted interest because of their technologically useful properties. The sol–gel route from alkoxide precursors[1] has been used to prepare such materials because it offers a low-temperature synthesis to materials with high purity and homogeneity. $(Ta_2O_5)_x(SiO_2)_{1-x}$ mixed oxides prepared this way possess high refractive indices rendering them suitable for optical components such as micro-lenses and optical fibres.[2] The high refractive index of a given sample has been shown to depend upon the level of atomic mixing of the two oxides, a property which in turn is sensitive to the exact method of synthesis. These materials also exhibit catalytic activity which derives from the acidity of the Ta–O–Si linkages present in their structures.[3] Again, preparation and composition are important in producing good catalysts with high surface areas and a high level of atomic mixing. In general, the useful properties of sol–gel derived $(Ta_2O_5)_x(SiO_2)_{1-x}$ mixed oxides are reduced by any phase separation of the two component oxides. Clearly, a sensible approach to optimizing the properties of these materials would be to study the atomic level structure in order to understand how the oxides mix from a structural point of view and to gain information on the mechanism of phase separation.

In this paper, the atomic structure of a series $(Ta_2O_5)_x(SiO_2)_{1-x}$ xerogels of various compositions and thermal histories have been studied using a comprehensive advanced methodology involving a combination of probe techniques.

Experimental

Sample preparation

The samples were prepared using the sol–gel route from the following precursors: tetraethyl orthosilicate, TEOS (Aldrich, 98%), and tantalum(v) ethoxide, $Ta(OEt)_5$, (Aldrich, 99.98%). HCl (Fisons) was used as a catalyst to promote the hydrolysis and condensation reactions and ethanol (Aldrich, 99.9%) was used as a mutual solvent.

The method of Yoldas[4] was used to promote homogeneity within the mixed oxide samples. This involved prehydrolysis of the TEOS to maximise the number of Si–OH groups before mixing with the more reactive $Ta(OEt)_5$ precursor; the aim being to encourage Ta–O–Si bonding as opposed to Ta–O–Ta bonding which could lead to phase separation. The chosen prehydrolysis conditions were TEOS : EtOH : H_2O in a 1 : 1 : 1 molar ratio in the presence of HCl (pH = 1), stirring for 2 hours. The appropriate quantity of $Ta(OEt)_5$ was then slowly added to the prehydrolysed TEOS solution while stirring. After allowing several minutes for the oxide precursors to mix, water was added such that the overall water : alkoxide molar ratio was 2. The resulting clear sol was then left to gel; this typically took a few days, depending on composition.

An amorphous tantulum oxide, a-Ta_2O_5, sample was also prepared so that the structural environment of Ta could be compared with that in the mixed oxides. This was prepared by slowly adding an acidified H_2O/EtOH (1 : 8 molar ratio) solution to an 0.5 M solution of $Ta(OEt)_5$ in EtOH while stirring.[5,6] A milk-white gel formed almost immediately.

It should be noted that all reagents were loaded in a dry box under a N_2 atmosphere and transferred using syringes to avoid absorption of moisture from the atmosphere. Samples for ^{17}O MAS NMR were prepared using 10 mol% ^{17}O enriched water (D-Chem).

All samples were aged for one week before being air dried for several days, finely ground and then pumped under vacuum for 24 hours to remove any excess solvent. Heat treatments were performed at a heating rate of 5 °C min^{-1} with each temperature maintained for 2 hours. Samples were prepared with nominal compositions of $(Ta_2O_5)_x(SiO_2)_{1-x}$ where $x=0.05$, 0.11, 0.18, 0.25 and each composition heated to 250, 500 and 750 °C. The a-Ta_2O_5 sample was calcined at 250 and 750 °C. ^{17}O enriched samples were prepared for the compositions $x=0.05$, 0.25 and 1. These enriched samples were heat treated at 125, 250, 350, 500 and 750 °C under a N_2 atmosphere in order to prevent the loss of ^{17}O.

FT-IR spectroscopy

Infrared spectra were recorded in diffuse reflectance mode on a Biorad FTS175C spectrometer controlled by Win-IR software. Samples were diluted (1 : 10 by weight) in dry KBr and scanned over the range 4000–400 cm^{-1} with a resolution of 4 cm^{-1}. Each spectrum was the result of summing 64 scans.

MAS NMR

The MAS NMR spectra were acquired on a Chemagnetics CMX300 Infinity spectrometer. The ^{29}Si spectra were collected at 59.6 MHz using MAS at typically 6 kHz with a 2.0 μs (~30° tip angle) pulse and a 20 s recycle delay. A 7.5 mm Chemagnetics double-bearing probe was used. The pulse delay was sufficient to prevent saturation. The spectra were referenced externally to Zeolite A (−89.7 ppm). Each spectrum was the result of summing ~3000 scans. The ^{17}O NMR spectra from the $(Ta_2O_5)_x(SiO_2)_{1-x}$ xerogels were collected at 40.7 MHz under MAS at typically 15 kHz with a recycle delay of 1–2.5 s using a Chemagnetics 4 mm double-bearing probe. The delay was sufficient to prevent saturation. A 90°–τ–180° echo sequence was applied with a short τ delay of 71.4 μs to overcome problems of probe ringing, thereby allowing the spectra to be phased correctly.

For the pure sol–gel prepared Ta_2O_5, the ^{17}O MAS NMR data were collected at a resonance frequency of 32.1 MHz using a Bruker 4 mm double-bearing MAS probe applying the same experimental approach and very similar conditions to those used for the mixed oxide gels.

All the ^{17}O MAS NMR spectra were referenced externally to H_2O (0 ppm). Typically each spectrum was the result of 50 000–100 000 co-added scans and took approximately 24 h to collect.

X-Ray diffraction

The powder X-ray diffraction pattern of the pure Ta_2O_5 xerogel heated to 750 °C was collected on a Philips PW1050 diffractometer using Cu-K_α radiation ($\lambda = 1.541$ Å). A range of $2\theta = 20$–$70°$ was scanned at a rate of $1° \text{ min}^{-1}$ with a step size of 0.02°. An estimate of particle size (S) was made using the Scherrer equation,[7] $S = K\lambda/\beta \cos\theta$, where K is a constant (0.89) and β is the full width at half height of a diffraction peak at angle θ.

EXAFS spectroscopy

Ta L_{III}-edge EXAFS data were collected in transmission mode at room temperature on station 7.1 at the Daresbury Laboratory SRS using a Si [111] crystal monochromator and 50% harmonic rejection. Ionisation chambers, filled with a mixture of Ar/He or Kr/He at appropriate partial pressures to optimise detector sensitivities, were placed in the beam path before and after the sample. Finely-ground samples were diluted in polyethylene (Aldrich, spectrophotometric grade) and pressed into pellets to give a satisfactory edge jump and absorption. Typically each EXAFS spectrum was the sum of three 45 min scans.

Results and data analysis

FTIR spectroscopy

Fig. 1(A) and (B) show the IR spectra of the $(Ta_2O_5)_x(SiO_2)_{1-x}$ xerogels unheated and after heating to 750 °C, respectively. Also shown, for comparison, is the spectrum from an α-Ta_2O_5 xerogel after heating to 250 °C. The peaks in these spectra have been assigned according to the literature.[8–12] The band at 3590 cm^{-1} is mainly due to stretching vibrations involving Si–OH groups and the band at 3350 cm^{-1} corresponds to adsorbed water. The band at 1610 cm^{-1} is assigned to the H–O–H bending vibration of water. The peaks at 1160, 1070 and 800 cm^{-1} are characteristic of a silica network: the bands at 1160 cm^{-1} and 1070 cm^{-1} are ascribed to the LO and TO components of the asymmetric stretch of the SiO_4 unit, respectively, and the feature at 800 cm^{-1} is due to the symmetric stretch of the SiO_4 unit. The band at about 960 cm^{-1} is best assigned to the stretching vibration of SiO^- groups[12] adjacent to different countercations; in this case, this band has contributions from both Si–OH and Si–O–Ta vibrations.

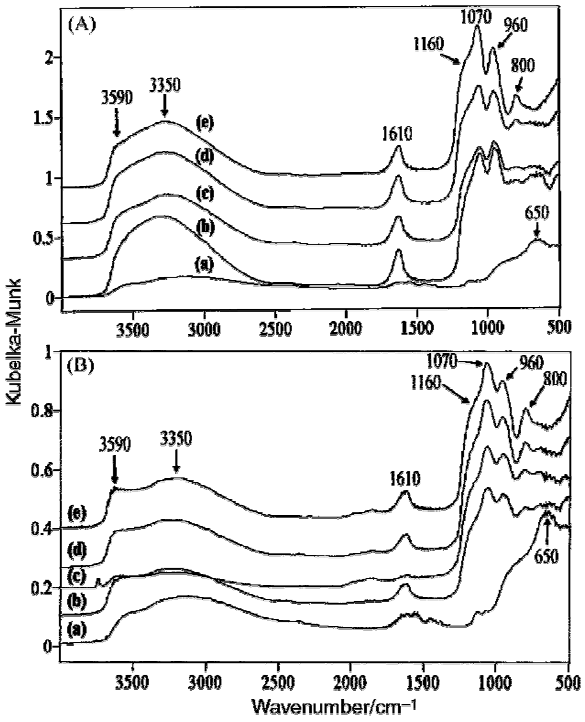

Fig. 1 (A) Infrared spectra of unheated $(Ta_2O_5)_x(SiO_2)_{1-x}$ xerogels: (b) $x = 0.25$, (c) $x = 0.18$, (d) $x = 0.11$ and (e) $x = 0.05$. The spectrum of an α-Ta_2O_5 xerogel heated to 250 °C (a) is shown for comparison. (B) Infrared spectra of $(Ta_2O_5)_x(SiO_2)_{1-x}$ xerogels after heating to 750 °C for 2 hours: (b) $x = 0.25$, (c) $x = 0.18$, (d) $x = 0.11$ and (e) $x = 0.05$. The spectrum of an α-Ta_2O_5 xerogel heated to 250 °C (a) is shown for comparison.

MAS NMR

The ^{29}Si MAS NMR spectra were deconvolved by Gaussian fitting using Spinsight 3.02 software; three signals could be distinguished at −93, −101 and −109 ppm with varying intensities. Each resonance represents a specific degree of Si–O–Si polymerisation. The −93 ppm signal comes from Si sites in a Q^2 configuration, and the −101 and −109 ppm signals come from Q^3 and Q^4 configurations, respectively (Q^n stands for a SiO_4 unit with n bridging oxygens[13]). The results of the Gaussian fitting are summarised in Table 1. Fig. 2 shows the ^{29}Si NMR data and peak deconvolution for the $(Ta_2O_5)_{0.05}(SiO_2)_{0.95}$ sample and clearly illustrates a shift to higher average Q species with heat treatment.

The ^{17}O MAS NMR spectra from pure Ta_2O_5 xerogels are shown in Fig. 3, and the major resonances listed in Table 2. In the dried, unheated xerogel two relatively narrow resonances at ~270 and ~430 ppm are observed along with some much broader underlying intensity that extends to ~0 ppm. On heating, the spectrum largely remains unchanged after heating up to 350 °C apart from a small positive shift of the peak that starts off at ~270 ppm (Table 2) and a change in the relative intensity. After heating to 500 °C there is a more significant change of the structure with some broader underlying intensity, and then at 750 °C the peak at 305 ppm becomes dominant.

The ^{17}O MAS NMR spectra of the enriched $(Ta_2O_5)_{0.05}(SiO_2)_{0.95}$ and $(Ta_2O_5)_{0.25}(SiO_2)_{0.75}$ samples are shown in Figs. 4 and 5, respectively, and the positions of the major resonances listed in Table 2. The spectra are dominated by a resonance which peaks at close to 0 ppm and shows structure at negative shift due to the quadrupole interaction.[14] This resonance is due to Si–O–Si bridges[15] with a contribution

Table 1 ^{29}Si NMR data[a] for $(Ta_2O_5)_x(SiO_2)_{1-x}$ xerogels

		Q^1			Q^2			Q^3			Q^4		
Sample	Heat Treatment/°C	fwhm/Hz	δ	I (%)	fwhm/Hz	δ	I (%)	fwhm/Hz	δ	I (%)	fwhm/Hz	δ	I (%)
$x=0.05$	none	—	—	—	520	−93.5	18	420	−101.2	40	610	−108.7	42
	250	—	—	—	640	−93.4	14	540	−100.8	37	640	−108.2	49
	750	—	—	—	600	−92.9	8	610	−101.2	23	730	−109.4	69
$x=0.11$	none	—	—	—	550	−93.3	26	470	−101.2	48	570	−108.9	26
	250	—	—	—	760	−93.3	25	630	−101.7	44	720	−109.6	31
	750	—	—	—	740	−93.1	12	680	−101.9	28	780	−109.3	60
$x=0.18$	none	—	—	—	810	−91.9	31	690	−100.6	51	860	−109.7	18
	250	—	—	—	910	−91.5	28	770	−101.4	51	800	−110.2	21
	750	—	—	—	620	−91.1	8	820	−103.2	49	900	−110.3	44
$x=0.25$	none	620	−83.0	8	630	−92.8	37	590	−100.9	42	630	−110.0	13
	250	—	—	—	850	−91.8	33	740	−101.0	54	830	−109.6	13
	750	—	—	—	810	−92.1	13	740	−101.9	54	740	−109.3	32

[a]fwhm, δ and I represent the line width, ^{29}Si chemical shift and relative intensity, respectively. Errors: fwhm ±25 Hz, δ ±0.5 ppm, I ±5%.

from Si–OH groups.[16] This signal has spinning sidebands from the MAS process at about 360 and −360 ppm. The resonances at ~285 and ~445 ppm observed for the $(TaO_5)_{0.25}(SiO_2)_{0.75}$ samples are at similar chemical shifts to those in the pure Ta_2O_5 xerogel and hence can be ascribed to Ta–O–Ta bonding. By comparison to the resonances due to Si–O–Si and Ta–O–Ta oxygen environments, the signal at around 160 ppm observed for both compositions has been ascribed to Ta–O–Si bridges. Both the Ta–O–Ta and Ta–O–Si resonances display a small change to higher chemical shift with increasing temperature of the heat treatment.

X-Ray diffraction

The powder X-ray diffraction pattern from the pure Ta_2O_5 xerogel heated to 750 °C indicates that crystallization has occurred by this calcination temperature. The powder pattern obtained matches the JCPDS card number 19-1299 for Ta_2O_5.

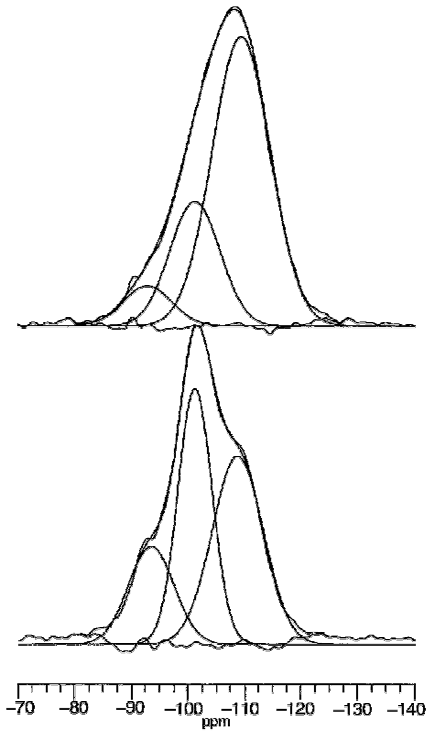

Fig. 2 ^{29}Si MAS NMR spectra showing deconvolution by Gaussian fitting for a $(Ta_2O_5)_{0.05}(SiO_2)_{0.95}$ xerogel in the unheated form (bottom) and after heat treatment to 750 °C.

An average particle size of ~400 Å was determined from the widths of the Bragg peaks using the Scherrer equation.

EXAFS spectroscopy

A heuristic version of the equation for the interpretation of EXAFS data is

$$\chi(k) = \mathrm{AFAC} \sum_j \frac{Nj}{kR_j^2} |f(\pi, k, R_j)| e^{-2R_j/\lambda(k)} e^{-2\sigma_j^2 k^2} \sin[2kR_j + 2\delta(k) + \psi(k, R_j)]$$

where $\chi(k)$ is the magnitude of the X-ray absorption fine structure as a function of the photoelectron wave vector k. AFAC is the proportion of electrons that perform an EXAFS-type scatter. N_j is the coordination number and R_j is the interatomic distance for the jth shell. $\delta(k)$ and $\psi(k,R_j)$ are the phase shifts experienced by the photoelectron, $f(\pi,k,R_j)$ is the amplitude of the photoelectron backscattering and $\lambda(k)$ is the electron mean free path; these are calculated within EXCURV98.[17] The Debye–Waller factor is $A=2\sigma^2$ in EXCURV98.

The programs EXCALIB, EXBACK and EXCURV98[17] were used to extract the EXAFS signal and analyse the data. Least squares refinements of the structural parameters of our samples were carried out against the k^3 weighted EXAFS signal

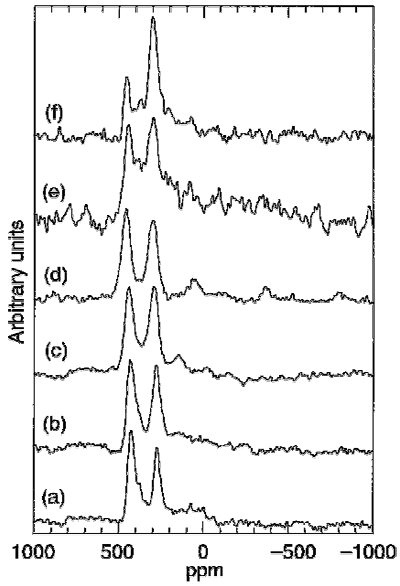

Fig. 3 ^{17}O MAS NMR spectra of various Ta_2O_5 samples: a) no heat treatment, b) 125 °C, c) 250 °C, d) 350 °C, e) 500 °C and f) 750 °C.

Table 2 ^{17}O MAS NMR chemical shifts

Sample	Heat treatment/°C	Peak positions/ppm (±5 ppm)			
Ta_2O_5 xerogel	none	428	272		
	125	434	280		
	250	441	295		
	350	457	300		
	500	445	298		
	750	455	305		
$(Ta_2O_5)_{0.25}(SiO_2)_{0.75}$	none	438	279	155	1
	125	431	280	161	1
	250	439	282	163	−2
	350	443	290	168	−4
	500	440	292	171	−7
	750	447	295	177	−4
$(Ta_2O_5)_{0.05}(SiO_2)_{0.95}$	none			141	−2
	125			145	−4
	250			150	−5
	350			147	−6
	500			155	−6
	750			156	−8

to minimise the fit index, FI,

$$FI = \sum_i [k^3(\chi_i^T - \chi_i^E)]^2$$

where χ_i^T and χ_i^E are the theoretical and experimental EXAFS, respectively. The results of the refinements are reported in terms of the discrepancy index, R_{di}.

$$R_{di}\ (\%) = \frac{\int |[\chi^T(k) - \chi^E(k)]| k^3\ dk}{\int |\chi^E(k)| k^3\ dk}$$

Crystalline Ta_2O_5, or tantite (Strem), was run as a reference material to check the validity of our data analysis and also to allow refinement of the parameter AFAC. The results obtained from this standard are summarised in Table 3. The parameters were obtained by fitting the EXAFS data over the range 2.5–16.0 $Å^{-1}$ (*i.e.* equivalent to 5–32 $Å^{-1}$ in conventional diffraction formalism). In these refinements, the coordination numbers were fixed at values consistent with the crystallographic data available.[18] It should be noted that the parameters derived from the crystallographic data included in Table 3 are much simplified: the crystal structure of tantite contains Ta atoms in thirteen inequivalent sites. The parameters shown are a weighted average over the 24 Ta atoms within the unit cell. Since the 13 Ta environments contain such a large range of Ta–O and Ta–Ta distances, only the three most significant shells have been used to model the EXAFS data: any other shells with $R > 4$ Å have such large Debye–Waller factors that they would not contribute significantly to the EXAFS

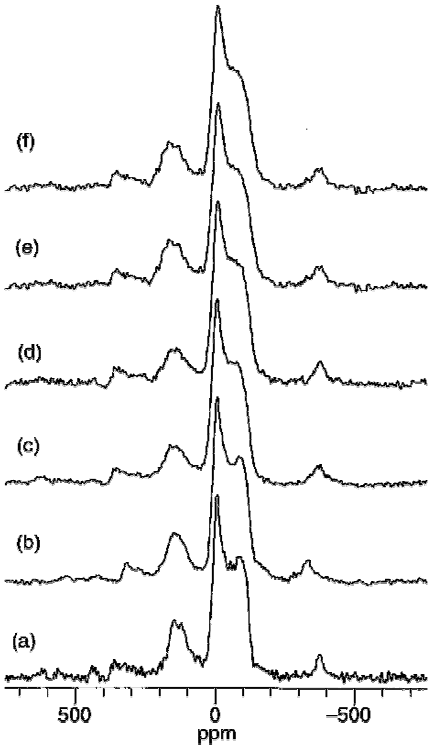

Fig. 4 ^{17}O MAS NMR spectra of a $(Ta_2O_5)_{0.05}(SiO_2)_{0.95}$ xerogel after various heat treatments: a) no heat treatment, b) 125 °C, c) 250 °C, d) 350 °C, e) 500 °C and f) 750 °C (peaks at 360 and −360 ppm are spinning side bands).

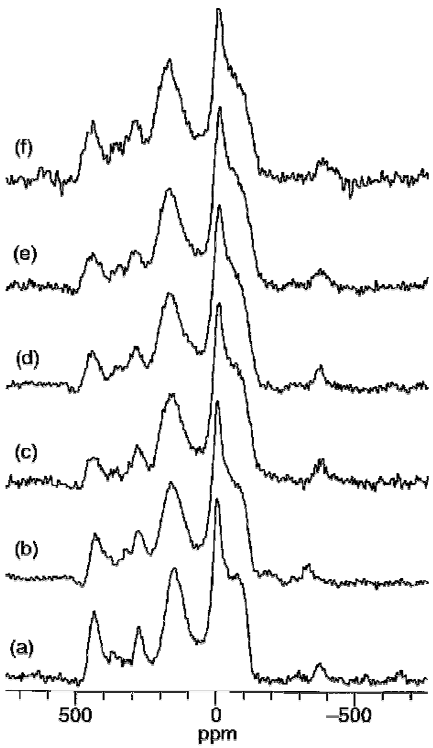

Fig. 5 ^{17}O MAS NMR spectra of a $(Ta_2O_5)_{0.25}(SiO_2)_{0.75}$ xerogel after various heat treatments: a) no heat treatment, b) 125 °C, c) 250 °C, d) 350 °C, e) 500 °C and f) 750 °C (peaks at 360 and −360 ppm are spinning side bands).

Table 3 Ta L_{III}-edge EXAFS derived structural parameters for reference compound, crystalline Ta_2O_5, and *a*-Ta_2O_5 xerogels. The parameters in italics have been fixed

Sample	Shell	*N*	*R*/Å	σ^2/Å^2	R_{di} (%)	Crystallographic data[18]
Crystalline Ta_2O_5	Ta–O	*5.6*	1.98(1)	0.021(1)	31	5.6O × 1.987 Å
	Ta–Ta	*3.7*	3.69(1)	0.012(1)		3.7Ta × 3.581 Å
	Ta–Ta	*3.6*	3.90(1)	0.009(1)		3.6Ta × 3.874 Å
a-Ta_2O_5 xerogel, unheated	Ta–O	4.7(3)	1.93(1)	0.015(1)	32	N/A
a-Ta_2O_5 xerogel, 250 °C	Ta–O	5.3(3)	1.93(1)	0.019(1)	32	N/A
Ta_2O_5 xerogel, 750 °C	Ta–O	5.8(4)	1.98(1)	0.023(2)	26	N/A
	Ta–Ta	1.3(4)	3.90(1)	0.018(7)		

signal. The errors are the statistical uncertainties calculated by EXCURV98; the real uncertainties will be higher. A value of 0.74 for AFAC was derived from the data from tantite; this was used throughout analysis of the data from our xerogel samples.

Also included in Table 3 are the structural parameters derived from the analysis of the Ta L_{III}-edge EXAFS data from the pure Ta_2O_5 xerogel both before and after heat treatment to 250 and 750 °C. The data for the unheated and 250 °C samples have been fitted using a single shell, *i.e.* one Ta–O correlation; attempts to fit a Ta–Ta shell resulted in an unrealistic distance. A two shell fit was used for the data from the 750 °C sample which exhibited a strong peak at ~3.9 Å in the Fourier transform. Fig. 6 shows the EXAFS data and their Fourier transform together with the calculated fit for the unheated *a*-Ta_2O_5 xerogel.

The EXAFS derived structural parameters for the $(Ta_2O_5)_x(SiO_2)_{1-x}$ xerogel samples are shown in Table 4. These data were best fitted with a model consisting of Ta–O and Ta–Si shells. The errors in Table 4 are the statistical uncertainties calculated by EXCURV98. Fig. 7 and 8 show the EXAFS data and their Fourier transforms together with the calculated fits for the two extremes of composition, $(Ta_2O_5)_{0.05}(SiO_2)_{0.95}$ and $(Ta_2O_5)_{0.25}(SiO_2)_{0.75}$, after heat treatment to 750 °C.

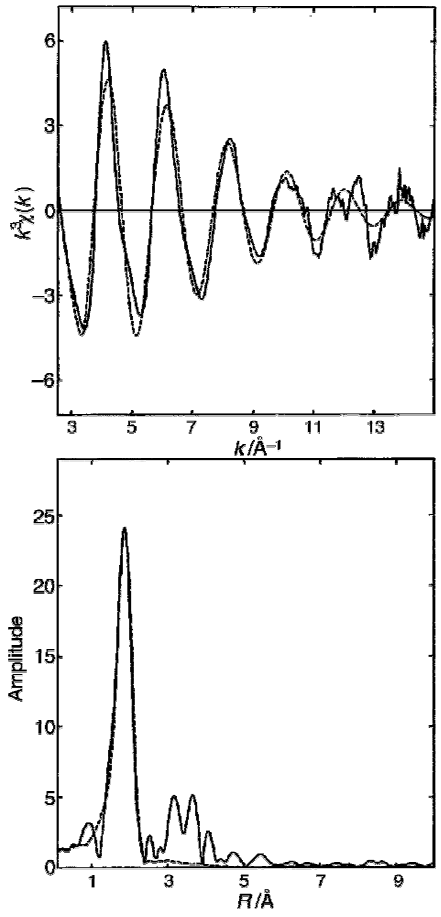

Fig. 6 Ta L_{III}-edge EXAFS data for unheated *a*-Ta_2O_5 xerogel: k^3 weighted EXAFS (top) and Fourier transform (bottom). Experimental data, solid line, and theoretical fit, dotted line.

Discussion

As can be seen from Table 1, the ^{29}Si MAS NMR results from the $(Ta_2O_5)_x(SiO_2)_{1-x}$ xerogels exhibit a general trend towards more polymerised Q^n species as the temperature of the heat treatment increases. This result is expected, since all the samples are composed predominantly of SiO_2 and it is well known that when a silica sol–gel is heated to progressively higher temperatures, further condensation and the resultant increase in cross-linking leads to an increase in the proportions of higher Q species. The point to note with these NMR results is the effect that Ta has on the distribution of silica Q species. Table 1 clearly shows that as the tantalum dopant level is increased, the extent of condensation of the silica network is reduced. This effect is very similar to that of Zr in $(ZrO_2)_x(SiO_2)_{1-x}$ sol–gels.[19–21] In such materials, the presence of silicon in $Si(SiO)_3(ZrO)$, $\{Q_{Zr}^3\}$ and $Si(SiO)_2(ZrO)_2$ $\{Q_{2Zr}^2\}$ environments contribute to the signals in the ^{29}Si NMR spectrum at −101 and −93 ppm, respectively. Zirconium clearly acts as a network modifier. This effect is due to the high field strength[22] of Zr^{4+} ions which causes them to adopt higher coordination numbers with respect to oxygen. Hence, Zr^{4+} cannot substitute tetrahedrally into the silica network. The behaviour of the Ta^{5+} in the samples studied here is also that of a network modifier with the NMR signals at −83, −93 and −101 ppm having contributions from $Si(SiO)(TaO)_3$, $\{Q_{3Ta}^1\}$, $Si(SiO)_2(TaO)_2$ $\{Q_{2Ta}^2\}$ and $Si(SiO)_3(TaO)$, $\{Q_{Ta}^3\}$. The overall trend in the data of a shift of the Q species distribution to more Q^1, Q^2 and Q^3 species with higher Ta concentration is a direct consequence of the network disrupting effect of Ta. This effect is emphasized by the widths of the NMR peaks which show a general increase with increasing Ta content.

The FTIR results shown in Fig. 1(A) and (B) give an insight into the interaction between the two oxides present in the $(Ta_2O_5)_x(SiO_2)_{1-x}$ xerogels. In both sets of spectra, the strengths of the silica network vibrations at 1160, 1070, and 800 cm^{-1} are reduced as the concentration of Ta is increased. This effect is most dramatic for the symmetric stretch of SiO_4[9] which is only just detectable in the $(Ta_2O_5)_{0.25}(SiO_2)_{0.75}$ sample both before heat treatment and after heating to 750 °C. The reduction in the strength of the silica network vibrations is due to the network modifying properties of Ta. These infrared results therefore support the conclusions drawn from the ^{29}Si NMR data.

The infrared results also yield qualitative information on the extent of Ta–O–Si bonding within the structures of these xerogels. This information can be derived by examining the absorption band at 960 cm^{-1} which is ascribed to a combination of Si–OH and Ta–O–Si vibrations. Considering the IR spectra from the unheated xerogels, with the exception of the $(Ta_2O_5)_{0.25}(SiO_2)_{0.75}$ sample, all of the samples contain similar amounts of hydroxyl groups, as seen from the intensities of the

Table 4 Ta L_{III}-edge EXAFS derived structural parameters for $(Ta_2O_5)_x(SiO_2)_{1-x}$ xerogels

Composition	Heat treatment/°C	Shell	N	R/Å	A/Å^2	R_{di} (%)
$(Ta_2O_5)_{0.25}(SiO_2)_{0.75}$	RT	Ta–O	4.8(2)	1.92(1)	0.011(1)	26
		Ta–Si	3.2(9)	3.30(1)	0.019(6)	
	250	Ta–O	4.9(2)	1.92(1)	0.013(1)	23
		Ta–Si	5.8(17)	3.32(2)	0.035(9)	
	750	Ta–O	4.6(2)	1.91(1)	0.014(1)	24
		Ta–Si	5.1(17)	3.31(2)	0.037(10)	
$(Ta_2O_5)_{0.18}(SiO_2)_{0.82}$	RT	Ta–O	4.8(2)	1.92(1)	0.011(1)	24
		Ta–Si	3.8(11)	3.30(1)	0.023(7)	
	250	Ta–O	4.8(2)	1.92(1)	0.011(1)	22
		Ta–Si	3.4(9)	3.30(1)	0.020(6)	
	750	Ta–O	4.4(2)	1.92(1)	0.012(1)	22
		Ta–Ta	2.7(8)	3.29(1)	0.020(6)	
$(Ta_2O_5)_{0.11}(SiO_2)_{0.89}$	RT	Ta–O	5.1(3)	1.92(1)	0.011(1)	24
		Ta–Si	1.8(6)	3.28(1)	0.007(4)	
	250	Ta–O	5.1(2)	1.92(1)	0.010(1)	22
		Ta–Si	2.8(7)	3.29(1)	0.015(4)	
	750	Ta–O	4.5(2)	1.92(1)	0.010(1)	20
		Ta–Si	2.6(7)	3.29(1)	0.016(5)	
$(Ta_2O_5)_{0.05}(SiO_2)_{0.95}$	RT	Ta–O	4.9(2)	1.93(1)	0.007(1)	25
		Ta–Si	2.1(6)	3.29(1)	0.007(4)	
	250	Ta–O	4.8(2)	1.92(1)	0.006(1)	20
		Ta–Si	2.3(6)	3.29(1)	0.009(3)	
	750	Ta–O	4.7(2)	1.92(1)	0.007(1)	19
		Ta–Si	2.0(5)	3.29(1)	0.009(3)	

bands at 3590 cm^{-1}. Hence, comparison of the intensities at 960 cm^{-1} should give an indication of the relative amount of Ta–O–Si bonding in each sample. Clearly, for the $x=0.05$, 0.11 and 0.18 samples, as the concentration of Ta increases so does the intensity of the 960 cm^{-1} band relative to the intensity of the SiO_2 network vibrations, thus suggesting an increase in the level of Ta–O–Si bonding. A similar trend can be observed for the xerogels after heating to 750 °C, with the exception of the $(Ta_2O_5)_{0.18}(SiO_2)_{0.82}$ sample which contains far fewer hydroxyl groups. The variation in intensity at 960 cm^{-1} with Ta

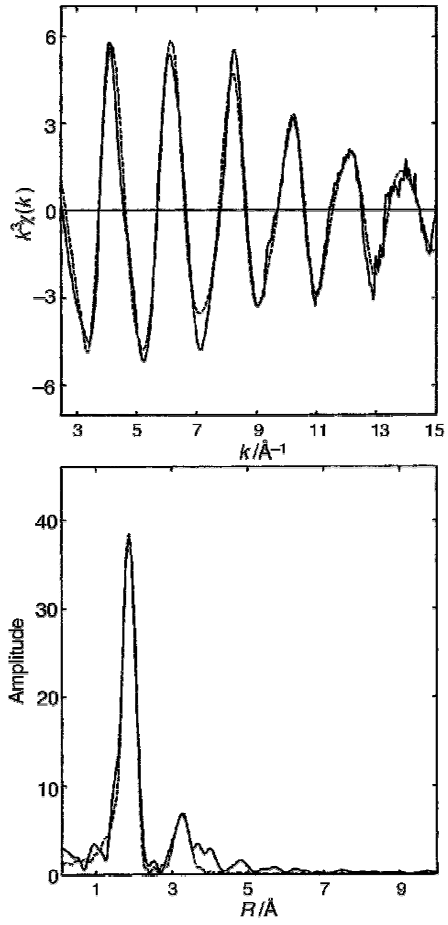

Fig. 7 Ta L_{III}-edge EXAFS data for $(Ta_2O_5)_{0.05}(SiO_2)_{0.95}$ after heat treatment to 750 °C: k^3 weighted EXAFS (top) and Fourier transform (bottom). Experimental data, solid line, and theoretical fit, dotted line.

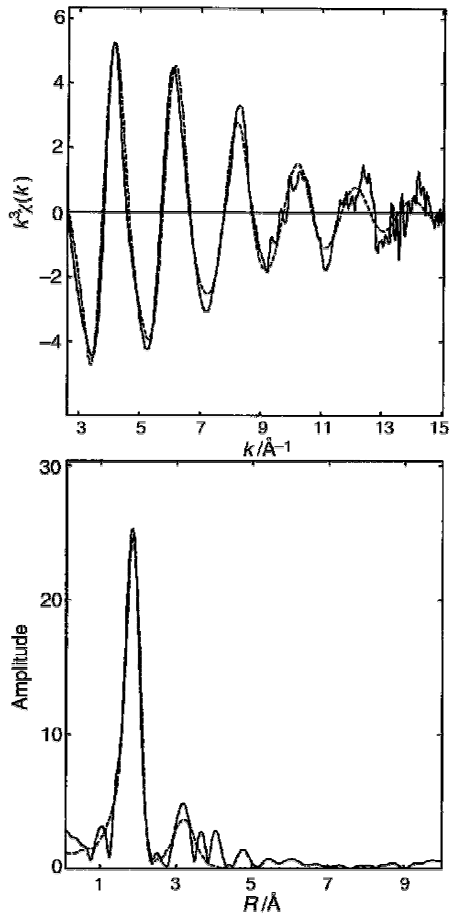

Fig. 8 Ta L_{III}-edge EXAFS data for $(Ta_2O_5)_{0.25}(SiO_2)_{0.75}$ after heat treatment to 750 °C: k^3 weighted EXAFS (top) and Fourier transform (bottom). Experimental data, solid line, and theoretical fit, dotted line.

concentration is not so pronounced for the heat treated xerogels. This suggests that for the higher concentrations not all of the Ta atoms are incorporated into the silica matrix. A possible reason for this is partial phase separation of the two components.

This hypothesis is supported by a comparison of the FTIR spectrum from the *a*-Ta_2O_5 xerogel with those from the $(Ta_2O_5)_x(SiO_2)_{1-x}$ samples. The band at 650 cm^{-1} in the spectrum from the *a*-Ta_2O_5 sample is clearly present in the spectra from the $(Ta_2O_5)_{0.25}(SiO_2)_{0.75}$ xerogel both before and after heating to 750 °C. This suggests that the $(Ta_2O_5)_{0.25}(SiO_2)_{0.75}$ xerogel contains a form of tantalum oxide which is very similar to *a*-Ta_2O_5, and hence provides evidence of phase separation in the highest Ta content xerogel. The IR spectra from the $(Ta_2O_5)_{0.18}(SiO_2)_{0.82}$ samples also exhibit a weak feature at 650 cm^{-1} which suggests that there is some degree of phase separation present in these samples, although not to the extent of the $(Ta_2O_5)_{0.25}(SiO_2)_{0.75}$ samples.

^{17}O MAS NMR shows two well defined, distinct oxygen coordinations in the pure *a*-Ta_2O_5 gel. With heat treatment there are at first some small changes in the relative proportions of these two environments. Also the chemical shifts of these two environments change which is probably related to subtle changes in the exact nature (*e.g.* the average bond length and/or angles) of these sites as the sample is heated. >From the known trends of the ^{17}O chemical shift it is probable that the peaks at ~270 and ~430 ppm correspond to local coordinations by *n* and *n*−1 tantalum atoms respectively. One of these environments is probably the same as occurs in the crystalline material where there are 34 oxygen environments of which approximately 60% can be designated OTa_3 and the remaining OTa_2.[18] On this basis we can assign the resonances at ~270 and ~430 ppm as those due to OTa_3 and OTa_2 configurations, respectively. The large difference in the intensities of the OTa_3 and OTa_2 peaks in the spectrum from the crystalline 750 °C sample where the two environments are known to be present in approximately 60/40 proportions, respectively, is probably due to a difference in ^{17}O quadrupolar coupling constants in the two environments. This observed behaviour in the pure oxide has some interesting similarities and differences to ^{17}O MAS NMR work on other simple pure oxides. TiO_2 gels are a mixture of OTi_3 and OTi_4 with heat treatment reducing the amount of OTi_4 until at the point of crystallisation it is eliminated altogether. In TiO_2 crystallisation is accompanied by a large reduction in the linewidth which is associated with a large decrease in the disorder on the OTi_3 sites.[23] Similar narrowing was also observed in the two sites of the monoclinic HfO_2 that forms on crystallisation.[24] The reduction in disorder on crystallisation in TiO_2 and HfO_2 reduces the chemical shift distribution that dominates the linewidth in the amorphous gel. Here the linewidth does not decrease much as the Ta_2O_5 xerogel crystallises, thus reflecting the high degree of atomic disorder in the crystalline state of Ta_2O_5.

The ^{17}O MAS NMR results from enriched $(Ta_2O_5)_{0.05}(SiO_2)_{0.95}$ and $(Ta_2O_5)_{0.25}(SiO_2)_{0.75}$ samples shown in Fig. 4 and 5, respectively, also yield information on the degree of atomic mixing of the two oxides. The spectra from the $(Ta_2O_5)_{0.05}(SiO_2)_{0.95}$ samples show clear resonances due to Si–O–Si (~0 ppm) and Ta–O–Si (160 ppm) bonding and an absence of resonances due to Ta–O–Ta bonding. These spectra are typical of those from an atomically mixed-oxide xerogel[19,25] and do not show any appreciable change occurring between the unheated sample and that preheated to 750 °C. The spectra from the $(Ta_2O_5)_{0.25}(SiO_2)_{0.75}$ samples exhibit two additional resonances at ~285 and ~445 ppm which have been ascribed to OTa_3 and OTa_2 environments, respectively. The observation and identification of these resonances is consistent with the conclusion drawn from the FTIR study that partial phase separation occurs within the $(Ta_2O_5)_{0.25}(SiO_2)_{0.75}$ samples. The only significant change in these spectra with heat treatment of the sample up to 750 °C is that the OTa_3 peak becomes more intense relative to the OTa_2 peak. This change is similar to that observed in the spectra from the pure Ta_2O_5 xerogels and suggests that the environment of the oxygen in the phase separated part of the $(Ta_2O_5)_{0.25}(SiO_2)_{0.75}$ sample becomes more like that in crystalline Ta_2O_5 with heat treatment. Despite phase separation, a strong resonance is still observed at 160 ppm for the $(Ta_2O_5)_{0.25}(SiO_2)_{0.75}$ samples indicating that a significant proportion of the tantala is atomically mixed with the silica. Similar behaviour has been observed in $(ZrO_2)_x(SiO_2)_{1-x}$ xerogels.[19]

The Ta L_{III}-edge EXAFS results presented here provide both detailed structural information of the Ta environment in an atomically mixed $(Ta_2O_5)_x(SiO_2)_{1-x}$ xerogel and yield qualitative information on the process of phase separation within this mixed oxide system. Concentrating first on the structural parameters obtained for the Ta–O correlation given in Table 4, it can be seen that on average for all samples, the Ta occupies an environment surrounded by five O atoms at a distance of 1.92 Å. This distance is in agreement with that of 1.920 Å predicted for five coordinate Ta^{VI} in an oxide using bond-valence parameters.[26] For all the samples, the nearest-neighbour environment of Ta does not appear to change with temperature. However, a structural change is observed across the composition range with the Debye–Waller factor, *A*, rising from ~0.007 $Å^2$ for the $(Ta_2O_5)_{0.05}(SiO_2)_{0.95}$ samples to ~0.013 $Å^2$ for the $(Ta_2O_5)_{0.25}(SiO_2)_{0.75}$ samples. This change reflects an increase in disorder in the Ta–O nearest-neighbour shell as the concentration of Ta is increased and is most probably due to partial phase separation which is accompanied by the presence of Ta with a coordination number of greater than 5. This observation is consistent with the results from the ^{17}O MAS NMR study which show the presence of OTa_3 configurations in the $(Ta_2O_5)_{0.25}(SiO_2)_{0.75}$ samples. The presence of OTa_3 must be accompanied by an increase in the average Ta–O coordination number, since from bond valence considerations, the presence of only five coordinate Ta would require only OTa_2 configurations.

The structural parameters in Table 4 obtained from fitting the second nearest-neighbour contributions to the EXAFS signal are less informative. Due to multiple scattering contribution at the second-shell distances, which have not been accounted for in this analysis, the parameters obtained should be treated as qualitative. The results for all samples suggest that the Ta second nearest-neighbour is Si at a distance of ~3.3 Å. This distance gives a Ta–O–Si angle of 137° which is entirely reasonable for a material which is predominantly an SiO_2 network with Ta dissolved in it; the Si–O–Si bond angle in silica being 146°.[27] Again, for all the samples except the ones with the highest loading of Ta, no significant structural evolution is observed in the second nearest-neighbour environment of Ta with increasing temperature of the heat treatment. The case of the $(Ta_2O_5)_{0.25}(SiO_2)_{0.75}$ samples is different. Examining the EXAFS data for the two extremes of composition, shown in Fig. 7 and 8, one can see there is a clear difference between the envelopes of the two sets of oscillations. Looking at the Fourier transforms one can observe a difference above 3 Å. In Fig. 8, for a $(Ta_2O_5)_{0.25}(SiO_2)_{0.75}$ xerogel heated to 750 °C, the match between the experimental and calculated Ta–Si peaks in the Fourier transform is poor, with the calculated peak being too wide. It is likely that the fitting procedure is trying to include contributions from other shells, possibly Ta–Ta, within this peak. Attempts to fit a Ta–Ta shell to the EXAFS data were unsuccessful, resulting in non-physical parameters. A similar situation occurred in the fitting of the data from the *a*-Ta_2O_5 samples where no meaningful structural parameters could be derived for the Ta–Ta correlations. It remains most probable that the poor modelling of the Ta–Si shell for the $(Ta_2O_5)_{0.25}(SiO_2)_{0.75}$ samples is due to a contribution from

Ta–Ta, resulting from a degree of phase separation, which cannot be modelled without the use of multiple scattering calculations (a highly non-trivial exercise for an amorphous, two-phase, material).

The Ta L_{III}-edge EXAFS derived structural parameters for the a-Ta_2O_5 shown in Table 3 offer an insight into the environment of Ta in this relatively poorly characterised material. For the unheated sample and that heated to 250 °C, the average coodination of Ta is close 5 with respect to oxygen with a Ta–O distance of 1.93 Å, whereas for the sample heated to 750 °C, the Ta–O coordination number and distance are closer to 6 and 2 Å, respectively. The latter result is expected since the XRD results show that crystallisation of the a-Ta_2O_5 occurs by 750 °C. The a-Ta_2O_5 samples both exhibit relatively large Debye–Waller factors of >0.015 Å^2 for the Ta–O shells which probably result from the presence of some Ta with a coordination number of greater than 5. This explanation is supported by the observation of OTa_3 enviroments with ^{17}O MAS NMR.

The observation that both the $(Ta_2O_5)_x(SiO_2)_{1-x}$ and a-Ta_2O_5 xerogels contain predominantly five-coodinated Ta is particularly interesting. This type of coordination of Ta with respect to oxygen is rare: $Ba_2Si_4Ta_6O_{23}$ was the first reported solid state compound with five coordinate tantalum.[28] However, five-coodinated Ta is perhaps more likely in amorphous network type structures, particularly in the case of the mixed tantala–silica xerogels where this type of coordination allows both the Ta–O and Si–O bonds to have a bond valence of one. In this way, inclusion of a small amount of tantala within the silica structure can occur whilst maintaining a network structure.

Conclusions

The first extensive structural characterisation of $(Ta_2O_5)_x(SiO_2)_{1-x}$ and a-Ta_2O_5 xerogels is presented here. EXAFS has allowed identification of five coordinate Ta in both these materials, a Ta environment which is extemely rare in the solid state. The FTIR and ^{17}O MAS NMR studies on the mixed oxides show that partial phase separation of the two component oxides starts to occur for $x>0.11$. Despite partial phase separation, the $(Ta_2O_5)_{0.25}(SiO_2)_{0.75}$ still contains extensive Ta–O–Si bonding, as shown by the ^{17}O MAS NMR results. ^{29}Si MAS NMR data have shown that the presence of Ta within the silica network reduces the connectivity of that network.

The result that partial phase separation can be detected in the $(Ta_2O_5)_x(SiO_2)_{1-x}$ xerogels using a widely available laboratory technique such as FTIR is particularly important because of the detrimental effect that segregation of the two component oxides has on the usefulness of these materials, can be routinely monitored.

Acknowledgements

The EPSRC is thanked for its support of the characterisation of sol–gel produced materials through grant GR/L28647 and for the funding of Dr G. Mountjoy through grant GR/K95987. MES thanks the EPSRC for the support of NMR instrumentation at the University of Warwick.

References

1 C. J. Brinker and G. W. Scherer, *Sol–Gel Science, The Physics and Chemistry of Sol–Gel Processing*, Academic Press, San Diego, 1990.
2 S. Satoh, K. Susa and I. Matsuyama, *J. Non-Cryst. Solids.*, 1992, **146**, 121.
3 G. Guiu and P. Grange, *J. Catal.*, 1995, **156**, 132.
4 B. E. Yoldas, *J. Non-Cryst. Solids*, 1980, **38**, 81.
5 T. Ohishi, S. Maekawa and A. Katoh, *J. Non-Cryst. Solids*, 1992, **147 & 148**, 493.
6 T. Hashimoto and T. Yoko, *Appl. Opt.*, 1995, **34**(16), 2941.
7 B. E. Warren, *X-Ray diffraction*, Dover, New York, 1990.
8 A. Bertoluzza, C. Fagnano and M. A. Morelli, *J. Non-Cryst. Solids*, 1982, **48**, 117.
9 M. C. Matos, L. M. Ilharco and R. M. Almeida, *J. Non-Cryst. Solids*, 1992, **147 & 148**, 232.
10 K. Nakamoto, *Infrared and Raman Spectra of Inorganic and Coordination Compounds, Part B*, Wiley-Interscience, New York, 1997.
11 G. Guiu and P. Grange, *Bull. Chem. Soc. Jpn.*, 1994, **67**, 2716.
12 B. Notari, *Adv. Catal.*, 1996, **41**, 253.
13 G. Engelhardt and D. Michel, *High resolution solid state NMR of silicates and zeolites*, Wiley, Chichester, 1987.
14 M. E. Smith, *Appl. Magn. Reson.*, 1993, **4**, 1.
15 M. E. Smith and H. J. Whitfield, *J. Chem. Soc., Chem. Commun.*, 1994, 723.
16 T. M. Walter, G. L. Turner and E. Oldfield, *J. Magn. Reson.*, 1988, **76**, 106.
17 N. Binstead, J. W. Campbell, S. J. Gurman and P. C. Stephenson, EXAFS analysis programs, Daresbury Laboratory, Warrington, 1991.
18 H. U. Hummel, R. Fackler and P. Remmert, *J. Chem. Ber.*, 1992, **125**, 551.
19 D. M. Pickup, G. Mountjoy, G. W. Wallidge, R. J. Newport and M. E. Smith, *Phys. Chem. Chem. Phys.*, 1999, **1**, 2527.
20 P. Tartaj, J. Sanz, J. Serna and M. Ocaña, *J. Mater. Sci.*, 1994, **29**, 6533.
21 M. Andrianainarivelo, R. Corriu, D. Leclercq, P. H. Mutin and A. Vioux, *J. Mater. Chem.*, 1996, **6**(10), 1665.
22 M. Nogami, *J. Non-Cryst. Solids*, 1985, **69**, 415.
23 T. J. Bastow, A. F. Moodie, M. E. Smith and H. J. Whitfield, *J. Mater. Chem.*, 1993, **3**, 697.
24 T. J. Bastow, M. E. Smith and H. J. Whitfield, *J. Mater. Chem.*, 1996, **6**, 1951.
25 D. M. Pickup, G. Mountjoy, G. W. Wallidge, R. Anderson, J. M. Cole, R. J. Newport and M. E. Smith, *J. Mater. Chem.*, 1999, **9**, 1299.
26 N. E. Brese and M. O'Keefe, *Acta Crystallogr., Sect. B*, 1991, **47**, 192.
27 D. I. Grimley, A. C. Wright and R. N. Sinclair, *J. Non-Cryst Solids*, 1990, **119**, 49.
28 J. Shannon and L. Katz, *J. Solid State Chem.*, 1970, **1**, 399.